Received: 7 June 2017 | Revised: 18 September 2017 | Accepted: 18 October 2017

DOI: 10.1002/jnr.24197

RESEARCH ARTICLE

WILEY

# Transplantation of feeder-free human induced pluripotent stem cell–derived cortical neuron progenitors in adult male Wistar rats with focal brain ischemia

Yulius Hermanto[1,2,3] | Tadashi Sunohara[1,2] | Ahmad Faried[3] | Yasushi Takagi[4] | Jun Takahashi[2] | Takakuni Maki[5] | Susumu Miyamoto[1]

[1]Department of Neurosurgery, Graduate School of Medicine, Kyoto University, Kyoto, Japan

[2]Department of Clinical Application, Center of iPS Cell Research and Application, Kyoto University, Kyoto, Japan

[3]Department of Neurosurgery, Faculty of Medicine, Universitas Padjadjaran, Bandung, Indonesia

[4]Department of Neurosurgery, Institute of Biological Sciences, Tokushima University, Tokushima, Japan

[5]Department of Neurology, Graduate School of Medicine, Kyoto University, Kyoto, Japan

**Correspondence**
Yasushi Takagi, Department of Neurosurgery, Institute of Biological Sciences, Tokushima University. 3-8-15, Kuramoto-cho, Tokushima, 770-8503, Japan.
Email: ytakagi@tokushima-u.ac.jp

**Funding Information**
This study was supported by a grant from the Network Program for Realization of Regenerative Medicine from the Japan Agency for Medical Research and Development and an Intramural Research Grant for Neurological and Psychiatric Disorders from the National Center of Neurology and Psychiatry.

## Abstract

The use of human induced pluripotent stem cells (hiPSCs) eliminates the ethical issues associated with fetal or embryonic materials, thus allowing progress in cell therapy research for ischemic stroke. Strict regulation of cell therapy development requires the xeno-free condition to eliminate clinical complications. Maintenance of hiPSCs with feeder-free condition presents a higher degree of spontaneous differentiation in comparison with conventional cultures. Therefore, feeder-free derivation might be not ideal for developing transplantable hiPSC derivatives. We developed the feeder-free condition for differentiation of cortical neurons from hiPSCs. Then, we evaluated the cells' characteristics upon transplantation into the sham and focal brain ischemia on adult male Wistar rats. Grafts in lesioned brains demonstrated polarized reactivity toward the ischemic border, indicated by directional preferences in axonal outgrowth and cellular migration, with no influence on graft survival. Following the transplantation, forelimb asymmetry was better restored compared with controls. Herein, we provide evidence to support the use of the xeno-free condition for the development of cell therapy for ischemic stroke.

**KEYWORDS**

cell therapy, human pluripotent stem cells, ischemic stroke, neural stem cells

## 1 | INTRODUCTION

Ischemic stroke gives rise to adult disability worldwide (George & Steinberg, 2015; Moskowitz, Lo, & Iadecola, 2010). Transplantation of human neural stem cells (NSCs) has been reported to improve functional recovery in animal models of stroke (Andres et al., 2011; Gomi et al., 2012; Mine et al., 2013; Oki et al., 2012; Tornero et al., 2013). Clinical trials of human NSC transplantation had been conducted in limited numbers of patients with few sensorimotor improvements (Kalladka et al., 2016; Kondziolka et al., 2005). Human induced pluripotent stem cells (hiPSCs) represent a valuable treatment option for stroke because the use of hiPSCs avoids many of the ethical issues associated with the use of fetal or embryonic material (Takahashi et al., 2007).

### Significance

Cortical neurons could be induced under the feeder-free condition from hiPSCs. The cells also could survive, migrate, differentiate, and undergo axonal outgrowth upon transplantation in adult male Wistar rats with focal brain ischemia.

  

Gray matter neuronal loss after stroke is irreplaceable because these neurons specifically develop during the embryologic period. Stroke increases neurogenesis of adult NSC niche and promotes migration of newly born neurons toward the ischemic side (Arvidsson, Collin, Kirik, Kokaia, & Lindvall, 2002). However, the neuronal identity is not like cortical neurons, as adult NSCs are physiologically programmed to produce olfactory bulb interneurons (Lledo, Merkle, & Alvarez-Buylla, 2008). Generation of cortical neuron progenitors from hiPSCs could overcome this hurdle for cellular replacement in stroke. The government agency addressed several issues on the clinical translation of cell therapy in stroke. One of those, development of cellular products without contamination of animal-derived materials, is strictly required. In the feeder-free condition, a higher concentration of exogenous basic fibroblast growth factor is required. The presence of spontaneously differentiated cells impairs the induction process. Therefore, feeder-free derivation might be not ideal for developing transplantable hiPSC derivatives (Meng, Liu, & Rancourt, 2011; Richards, Fong, Chan, Wong, & Bongso, 2002; Zhang et al., 2016).

Therefore, we evaluated the differentiation outcome of hiPSC-derived cortical neuron progenitors under the feeder-free condition and transplanted the cells in the subacute period (1 week) post reperfusion to investigate in vivo differentiation and the therapeutic potential.

## 2 | MATERIALS AND METHODS

### 2.1 | Cortical neuronal progenitor differentiation

Kyoto University Graduate School of Medicine authorized the use of the human material. HiPSC (836B1) was established from dermal fibroblast of a healthy volunteer (developed by CiRA, Kyoto University) and previously maintained in the SNL feeder condition. In this study, we maintained on laminin E8 fragment (iMatrix 511, Nippi, Ibaraki, Japan) with feeder-free culture medium (Stemfit [AKO3], Ajinomoto, Tokyo, Japan). To adjust the differentiation in the feeder-free condition, we modified a previously described protocol on SNL feeder condition (Motono et al., 2016). Confluent hiPSC colonies were pretreated with Y-27632 15 μM (WAKO, Tokyo, Japan) prior to differentiation. The colonies were dissociated with Accumax (Innovative Cell Tech., San Diego, CA, USA), and 12,000 live cells per well were then allowed to form embryoid body–like aggregates in U-bottom 96-well plates (Sumitomo Bakelite). To adjust the induction in the feeder-free condition, we modified a previously described protocol on the SNL feeder condition (Motono, Ioroi, Ogura, & Takahashi, 2016). The colonies were dissociated with Accumax (Innovative Cell Tech., San Diego, CA, USA), and 12,000 live cells per well were then allowed to form embryoid body–like aggregates in U-bottom 96-well plates (Sumitomo Bakelite, Kobe, Japan). The neural induction medium contained Dulbecco's modified Eagle medium/F-12 (WAKO, Tokyo, Japan), 20% knockout serum replacement, nonessential amino acids (0.1 mM), $_{L}$-glutamine (2 mM; Gibco, Tokyo, Japan), and 2-mercaptoethanol (0.1 mM; WAKO, Tokyo, Japan). Neurobasal medium + B27 (Gibco, Tokyo, Japan) was used for neuronal differentiation. Small molecule compounds: C59 (10 nM; Cellagen Tech., San Diego, CA, USA), LDN193189 (100 nM; Stemgent, Beltsville, MD, USA), SB431542 (10 μM; Sigma Aldrich, Osaka, Japan), Y-27632 (50 μM; WAKO, Tokyo, Japan), and bFGF (5 ng/ml; Life Technologies, Tokyo, Japan). For transplantation, day 25 aggregates of differentiated hiPSCs were collected and dissociated using a neural tissue dissociation kit (MB-X9901, Sumitomo Bakelite, Kobe, Japan) and then resuspended at 50,000 cells per microliter. Some cells were replated (100,000 cells/cm$^2$) on precoated dishes with poly-L-ornithine (15 μg/ml), laminin (0.45 μg/ml), and fibronectin (2 μg/ml) for assessment of in vitro maturation.

### 2.2 | Quantitative polymerase chain reaction

RNA was purified from the cell culture with RNeasy Plus Mini Kit (Qiagen, Hilden, Germany) per the manufacturer's instructions. cDNA was constructed from the extracted RNA with SuperScript III Reverse Transcriptase (Invitrogen). Quantitative polymerase chain reactions were carried out with the Thermal Cycler Dice Real Time System (Takara Bio Inc., Shiga, Japan). The data were assessed by using a ΔCT method and normalized to *GAPDH* expression. Experiments were independently quadruplicated. The primers were listed in Table 1.

### 2.3 | Animals and cell transplantation

The Institutional Animal Care Committee of the Kyoto University Graduate School of Medicine approved all protocols. The Animal Facility of

**TABLE 1** Primers list

| | Gene | Forward (5′-3′) | Reverse (5′-3′) |
|---|---|---|---|
| 1 | *CTIP2* | GAGTACTGCGGCAAGGTGTT | TAGTTGCACAGCTCGCACTT |
| 2 | *FOXG1* | ACAAGGTGTGGAGTGTCAGC | GCACACATGGAAATCTGGCG |
| 3 | *GAPDH* | GGTCGGAGTCAACGGATTTG | TCAGCCTTGACGGTGCCATG |
| 4 | *LHX2* | GCGACACCGAGACGACCAT | GAACAGGTGAGCTCCGACT |
| 5 | *POUF51* | AGACCATCTGCCGCTTTGAG | GCAAGGGCCGCAGCTT |
| 6 | *NANOG* | GGCTCTGTTTTGCTATATCCCCTAA | CATTACGATGCAGCAAATACGAGA |
| 7 | *PAX6* | GTGTCTACCAACCAATTCCACAAC | CCCAACATGGAGCCAGATG |
| 8 | *TBR1* | ATGGGCAGATGGTGGTTTTA | GACGGCGATGAACTGAGTCT |

Kyoto University Center for iPS Cell Research and Application provided husbandry services in the specific pathogen-free facility for all animals used in research. Adult male Wistar rats (RRID: RGD_2314928; Shimizu Laboratory Supplies; $n = 35$; 250–280 g; 12–13 weeks old) were studied. Rats were randomly allocated into sham ($n = 10$), vehicle ($n = 12$), and transplantation ($n = 13$). The anesthetic regime was isoflurane (1.5%) in a mixture of $O_2$ and $N_2O$ (30%:70%, vol:vol). A 5-0 silicone-coated nylon thread (Doccol Co., MA, USA) was inserted into the right internal carotid artery through a small incision in the common carotid artery toward the carotid end ($\pm$ 18 mm) (Takagi et al., 1998). The thread was left in place for 90 min and retrieved afterward to allow reperfusion. Body temperature was maintained in the normothermic range (37 °–38 °C) with a feedback-controlled heating pad and incubator (Biomachinery Co., Chiba, Japan). Rats that died within 48 hr after ischemia were excluded from the rest of the study (vehicle = 2, transplantation = 3). Cell transplantation was performed with stereotactic injection of $5 \times 10^4$ cells in 1 μl (0.5 μl/min) through a 26G needle into the right cortex (from the bregma: A, + 0.5; L, + 1.5; and V, −1.9 mm). Both the sham ($n = 10$) and transplantation ($n = 10$) group underwent transplantation. All rats received cyclosporine A 10 mg/kg/day subcutaneously from the day of transplantation to the day of sacrifice for immunosuppression (4 weeks post transplantation). Animals were euthanized with pentobarbital and perfused transcardially with 4% paraformaldehyde. The brains were cut at 30-μm thickness with a cryostat.

## 2.4 | Immunostaining

Cells were fixed in 4% paraformaldehyde for 15 min at room temperature. Aggregates were cryosectioned at 12 μm. Primary antibodies (Table 2) were diluted in blocking solution and incubated overnight at 4 °C. Alexa fluorescent-conjugated (Life Technologies, Tokyo, Japan) donkey antibodies (1:500) were used as secondary antibodies. Slides were mounted with Prolong Gold Antifade (Life Technologies, Tokyo, Japan). Fluorescent images were obtained using a BZ-X710 microscope (Keyence, IL, USA).

## 2.5 | Axonal density measurement

The axonal outgrowth was evaluated by anti-human neural cell adhesion molecule (NCAM, 1:500, Santa Cruz, sc-106, RRID: AB_627128) staining after amplification with TSA-fluorescein (Perkin Elmer, MA, USA) per manufacturer's instructions. Human NCAM was inspected according to the destined regions: ipsilateral corpus callosum, ipsilateral striatum, contralateral corpus callosum, and lateral septal nuclei. The images were analyzed with NIH Image J (RRID: SCR_003070). The fibers' optical density was normalized to the intensity of the graft core.

**TABLE 2** Antibody ID

| Antibody ID | Antibody name | Target antigen | Vendor cat. no. | Clonality | Clone ID | Host | Concentration |
|---|---|---|---|---|---|---|---|
| AB_2064130 | Ctip2 antibody [25B6] - ChIP Grade | BCL11B human, mouse | Abcam ab18465 | Monoclonal | 25B6 | Rat | 1:1,000 |
| AB_1860617 | Ctip2 antibody | Human Ctip2 | Abcam ab82701 | Polyclonal | | Rabbit | 1:400 |
| AB_2088491 | Doublecortin (N-19) antibody | DCX human, rat, mouse | Santa Cruz Biotechnology sc-8067 | Polyclonal | N-19 | Goat | 1:500 |
| | Anti-Human/ Mouse Bf1 | Brain factor 1 human, mouse | Takara Bio Inc M227 | Polyclonal | | Rabbit | 1:1,000 |
| AB_641021 | GFAP (C-19) antibody | GFAP human, mouse, rat | Santa Cruz Biotechnology sc-6170 | Polyclonal | C-19 | Goat | 1:500 |
| AB_627128 | Mouse Anti-Human NCAM (ERIC 1) Monoclonal, Unconjugated, Clone Eric 1 antibody | Human NCAM1 | Santa Cruz Biotechnology sc-106 | Monoclonal | ERIC1 | Mouse | 1:500 |
| AB_2251134 | Anti-Nestin, clone 10C2 antibody | Nestin human | Millipore MAB5326 | Monoclonal | 10C2 | Mouse | 1:500 |
| AB_94090 | Human Nuclei antibody | ND | Millipore MAB1281 | Monoclonal | | Mouse | 1:500 |
| AB_839504 | Anti-Iba-1 Polyclonal Antibody | Iba-1 | Wako 019-19741 | Polyclonal | | Rabbit | 1:500 |
| AB_2135660 | LHX2 (C-20) antibody | LHX2 human, mouse, rat | Santa Cruz Biotechnology sc-19344 | Polyclonal | C-20 | Goat | 1:100 |

(Continues)

**TABLE 2** (Continued)

| Antibody ID | Antibody name | Target antigen | Vendor cat. no. | Clonality | Clone ID | Host | Concentration |
|---|---|---|---|---|---|---|---|
| AB_92184 | Rabbit Anti-Musashi Polyclonal antibody | Musashi human, mouse, rat | Millipore AB5977 | Polyclonal | | Rabbit | 1:500 |
| AB_355097 | Human Nanog Affinity Purified Polyclonal Ab antibody | Human Nanog Affinity Purified Abhuman | R and D Systems AF1997 | Polyclonal | | Goat | 1:400 |
| AB_262097 | Mouse Anti-N-Cadherin Monoclonal Antibody | N-Cadherin chicken/avian, human, mouse, rabbit, rat, simian, human, monkey | Sigma-Aldrich C3865 | Monoclonal | GC-4 | Mouse | 1:500 |
| AB_653551 | Oct-3/4 (N-19) antibody | POU5F1 human, mouse, rat | Santa Cruz Biotechnology sc-8628 | Polyclonal | N-19 | Goat | 1:500 |
| AB_628051 | Oct-3/4 (C-10) antibody | POU5F1 human, mouse, rat | Santa Cruz Biotechnology sc-5279 | Monoclonal | C-10 | Mouse | 1:500 |
| AB_10715442 | Pax-6 antibody | Pax-6 human | BD Biosciences 561462 | Monoclonal | | Mouse | 1:300 |
| AB_310177 | Rabbit Anti-Histone H3, phospho (Ser10) Mitosis marker Polyclonal antibody | Histone H3, phospho (Ser10) bovine, canine, chicken/avian, donkey, drosophila, feline, guinea pig, hamster, horse, human, mouse, other, porcine, rabbit, rat, sheep, simian, xenopus, drosophila, vertebrates | Millipore 06-570 | Polyclonal | | Rabbit | 1:500 |
| AB_2239879 | Human SOX1 Affinity Purified Polyclonal antibody | SOX1 human | R and D Systems AF3369 | Polyclonal | | Goat | 1:500 |
| AB_11213568 | Anti-Stage-Specific Embryonic Antigen-4 | Stage-Specific Embryonic Antigen-4 human, mouse | Millipore MAB4304 | Monoclonal | MC-813-70 | Mouse | 1:500 |
| AB_2200219 | TBR1 antibody | Tbr1 human, mouse | Abcam ab31940 | Polyclonal | | Rabbit | 1:1,000 |
| AB_2119183 | Mouse Anti-TRA-1-60 Monoclonal antibody | TRA-1-60 human | Millipore MAB4360 | Monoclonal | TRA-1-60 | Mouse | 1:500 |
| AB_663339 | Rabbit Anti-Neuronal Class III beta-Tubulin Purified Monoclonal Antibody | Neuronal Class III beta-Tubulin | Covance Research Products Inc MRB-435P-100 | Monoclonal | Tuj1 | Rabbit | 1:500 |
| AB_2313773 | Neuronal Class III beta-Tubulin (TUJ1) | Neuronal Class III beta-Tubulin (TUJ1) Purified | Covance Research Products Inc MMS-435P | Monoclonal | Tuj1 | Mouse | 1:500 |

(Continues)

**TABLE 2** (Continued)

| Antibody ID | Antibody name | Target antigen | Vendor cat. no. | Clonality | Clone ID | Host | Concentration |
|---|---|---|---|---|---|---|---|
| | | mammalian, other mammalian, hamster, sheep, bovine, horse, rabbit, guinea pig, human, non-human primate, donkey, feline, goat, porcine, canine, mouse, rat | | | | | |
| AB_882455 | Mouse Anti-Human SATB2 Monoclonal Antibody | Human SATB2, reacts with human, mouse | Abcam ab51502 | Monoclonal | SATBA4B10 | Mouse | 1:500 |

## 2.6 | Behavior testing

Behavior was tested preoperatively for baseline and repeated weekly for 4 weeks post stroke by an investigator blinded to treatment ($n = 10$ per group). Animals were randomized at 1 week post infarction to receive either transplantation (MCAO) or vehicle. (i) Vibrissae-elicited forelimb placing test: 10 trials of the vibrissae-evoked forelimb placing test were carried out on each side as described previously (Woodlee et al., 2005); (ii) cylinder test (Schallert, Fleming, Leasure, Tillerson, & Bland, 2000): rats were placed in a glass cylinder, and the number of times they reared and touched the cylinder in a weight-bearing fashion with the left, right, or both forelimbs was counted for 20 hits. The left: right ratio was calculated.

## 2.7 | Statistical analysis

Statistical analysis was performed using GraphPad Prism 7 (RRID: SCR_002798). On the basis of the previous study (Gomi et al., 2012), we calculated that at least 8 animals were needed for statistical analysis. Histological data were analyzed by *t* test. The behavioral data were analyzed with a 2-way ANOVA followed by a Tukey post hoc test for multiple comparisons. Differences were considered significant at

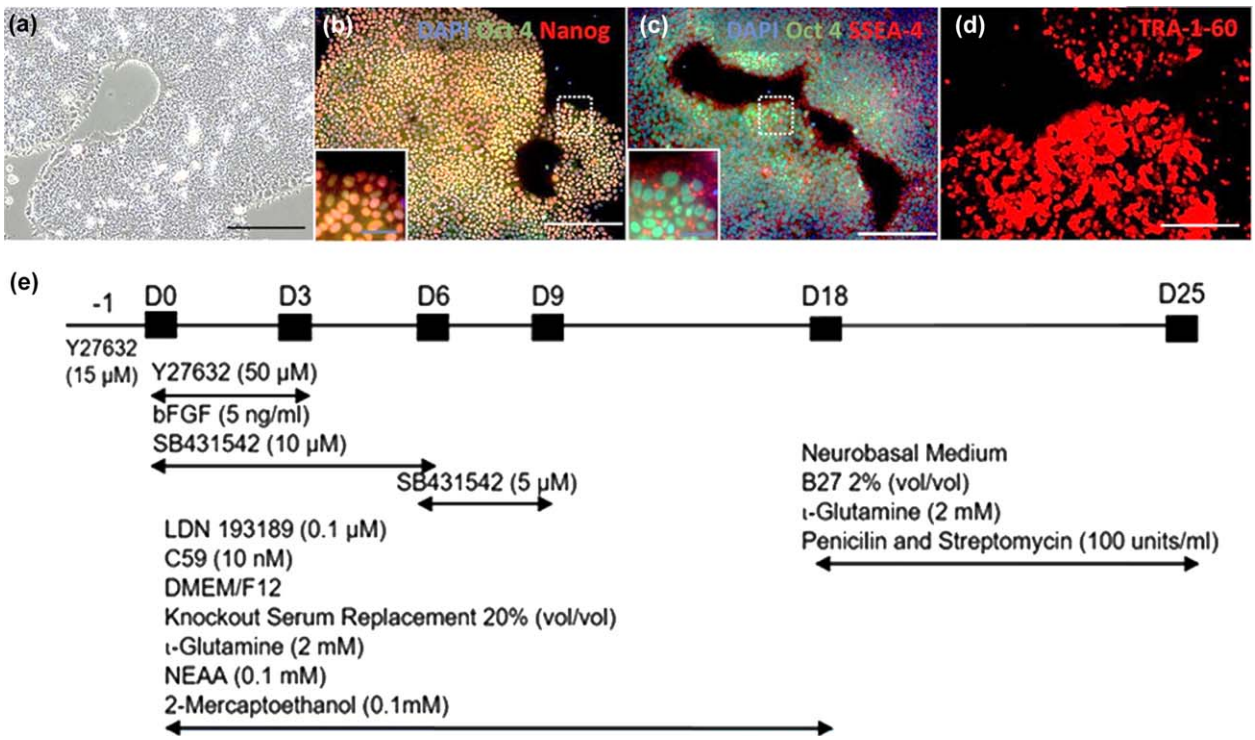


**FIGURE 1** Feeder-free maintenance of hiPSCs (836B1). (a) Rounded colonies' morphology without evidence of spontaneously differentiated cells. (b–d) Pluripotency markers (Oct 4, Nanog, SSEA-4, and TRA-1-60) were expressed in all cells. White boxes show higher magnifications of areas indicated by white dashes. (e) Simplified diagram of differentiation protocol. White/black scale bars: 100 μm; blue scale bar: 50 μm. [Color figure can be viewed at wileyonlinelibrary.com]

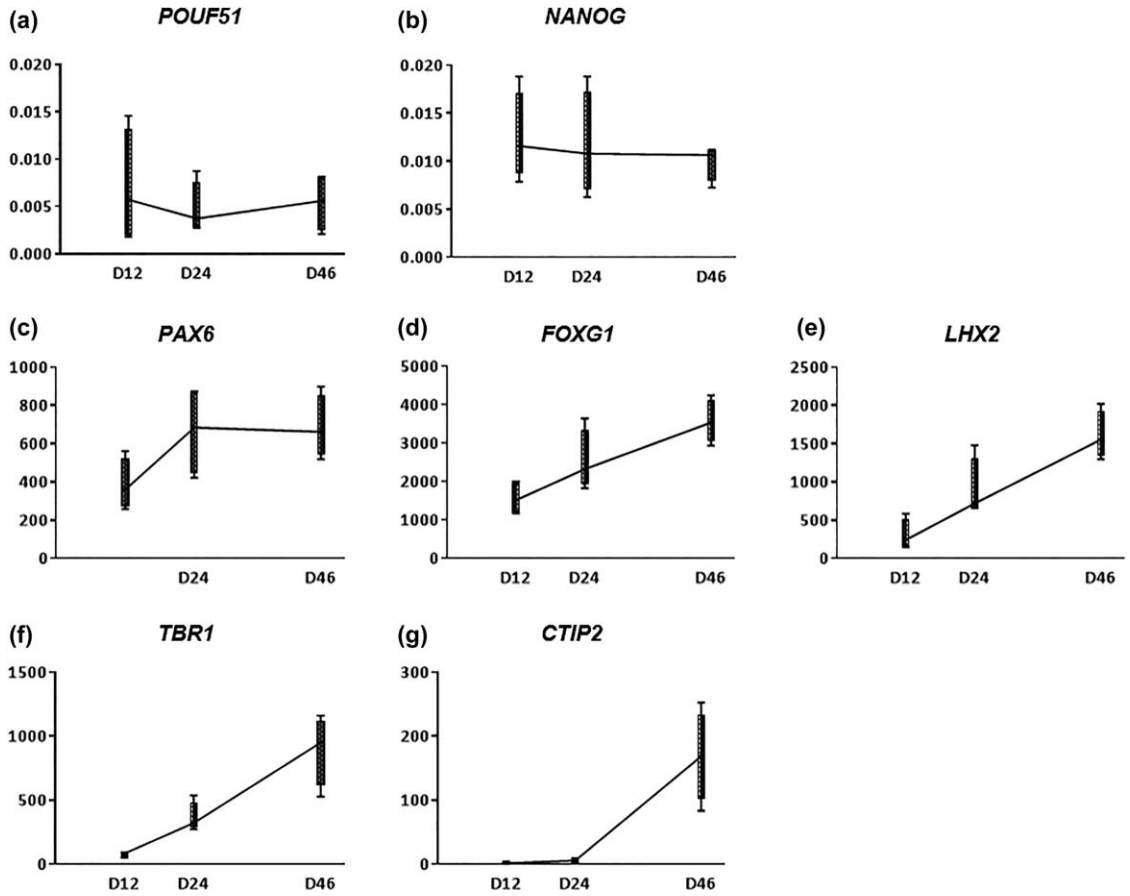


**FIGURE 2** Quantitative polymerase chain reaction of representative gene expression during in vitro differentiation. (a,b) Pluripotent-related genes (*POUF51* and *NANOG*) were downregulated. (c–e) Telencephalon and pallium-related markers (*PAX6*, *FOXG1*, and *LHX2*) were upregulated. (f,g) Expression of postmitotic deep layer neuron markers (*TBR1* and *CTIP2*) of the neocortex was detected. The graphs represent whisker box plot ($n = 4$)

$p < .05$. Graphs represent whisker box plots. Values are presented as mean ± *SEM*.

## 3 | RESULTS

### 3.1 | Generation of feeder-free cortical neuron progenitor cells

We adapted our clinical grade protocol for dopaminergic neuron differentiation (Doi et al., 2014) into cortical neuron progenitors. To remove animal-derived contamination, we further cultured hiPSCs (836B1) on laminin E8-511 fragment. The pluripotent-related markers of hiPSCs (Oct 3/4, Nanog, SSEA-4, and TRA-1-60) were retained in all colonies (Figure 1a–d). We employed a combination of dual-SMAD and Wnt inhibition for induction of cortical neuron progenitor with embryoid body–like aggregate (Figure 1e). The downregulation of pluripotent genes (*POUF51* and *NANOG*) and upregulation of dorsal pallium-related genes (*PAX6*, *FOXG1*, and *LHX2*) represented the induction process (Figure 2a–e). Over the time of differentiation, the deep layer neuron markers (*TBR1* and *CTIP2*) of the neocortex were detected (Figure 2f,g).

The cellular aggregate self-organized into rosette formation upon culture (Figure 3a), which characterized the neuronal induction. The success of induction was confirmed by detection of telencephalon progenitor marker (FoxG1) and neocortex progenitor markers (Lhx2 and Pax6) (Figure 3b). The rosette structure was confirmed as neuroepithelial (Nestin, Sox1, and N-Cadherin), served as the mitotic center, and retained expression of neocortex markers (FoxG1 and Lhx2) (Figure 3c–f). Postmitotic deep layer neurons (Tbr1 and Ctip2) of neocortex were observed at the periphery of the progenitor zone (Figure 3g,h). Upon dissociation and attachment culture, immature cortical neurons were observed (Figure 3i–l). The differentiation into astrocytes (GFAP) was observed upon long-term culture (> 80 days, Figure 3m). In this condition, there was no differentiation into oligodendrocyte lineages at least until 90 days in vitro.

### 3.2 | Graft characteristics

Graft survival was indistinct between the sham and MCAO group (8,358 ± 2,602 and 11,404 ± 3,982, respectively, $p = .53$, *t* test, Figure 4a). Transplanted grafts in the MCAO group exhibited more lateral migration toward the ischemic border (0.84 ± 0.14 and 26.12 ± 1.52, respectively, $p < .0001$, *t* test, Figure 4b). Grafts were similar in sham and MCAO, consisted of immature neurons ($Tuj1^+/HuNuc^+$), and were surrounded by host gliosis ($GFAP^+/HuNuc^-$) (Figure 5a–d). Migrating

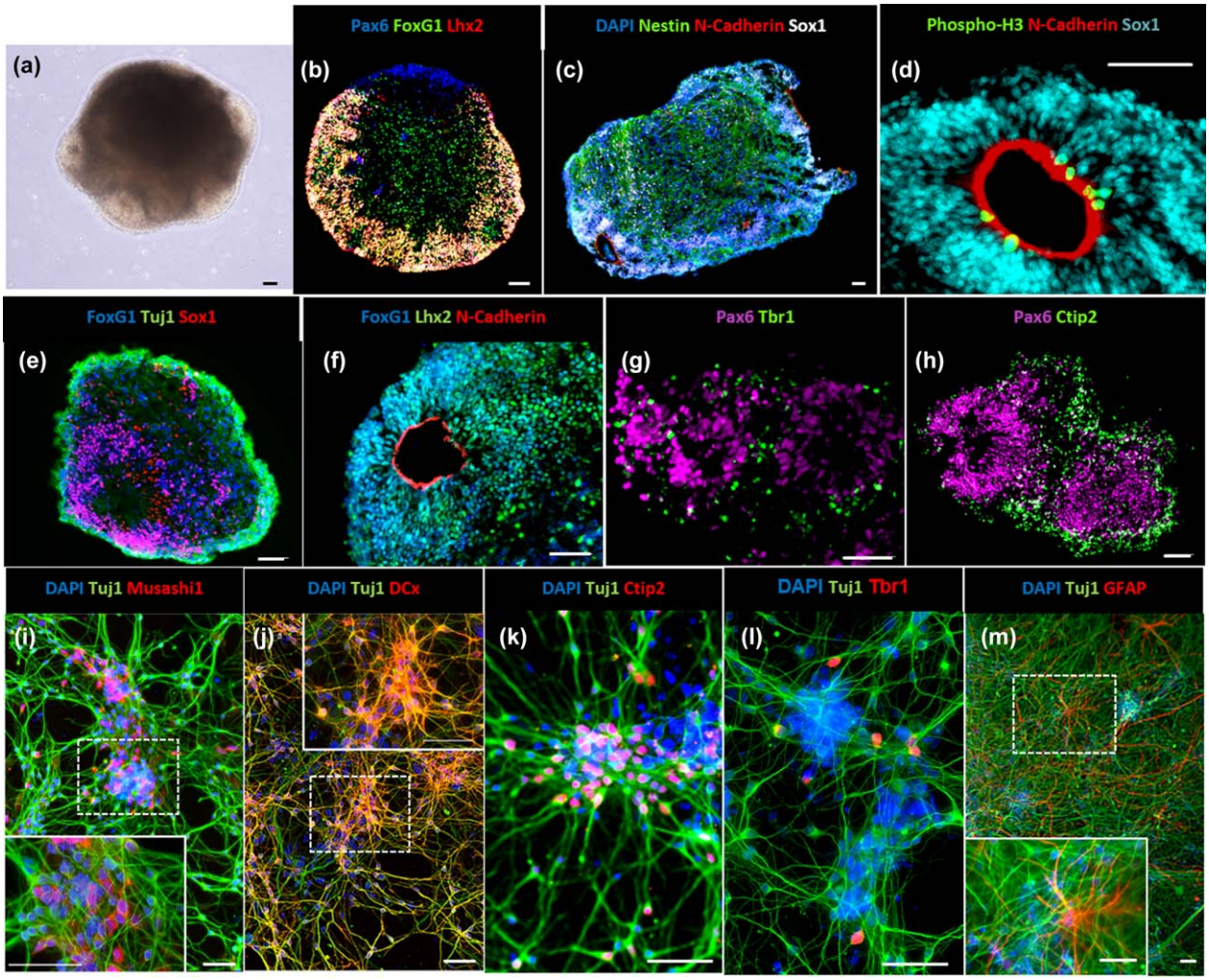


**FIGURE 3** Microscopy examination of the differentiated cells. (a) Phase contrast of the sphere on day 46. (b) On day 25 of differentiation, neocortex progenitors (FoxG1$^+$ and Lhx2+) were induced. (c) On day 46 of differentiation, neuroepithelial cells were self-organized into rosette structure. (d) The rosette structure served as the mitotic center. (e,f) The progenitor zone expressed FoxG1 and Lhx2. (g,h) Deep layer neurons (Ctip2 and Tbr1) of the neocortex were observed in the periphery of the rosette. (i,j) Immature neuron morphology and markers (Tuj1 and DCx) were observed. (k,l) The neuronal identities were the deep layer of the neocortex (Tbr1 and Ctip2). (m) On day 81 of differentiation, astrocytic differentiation was observed (GFAP). White boxes show higher magnification of areas indicated by white dashes. Scale bars: 50 μm. [Color figure can be viewed at wileyonlinelibrary.com]

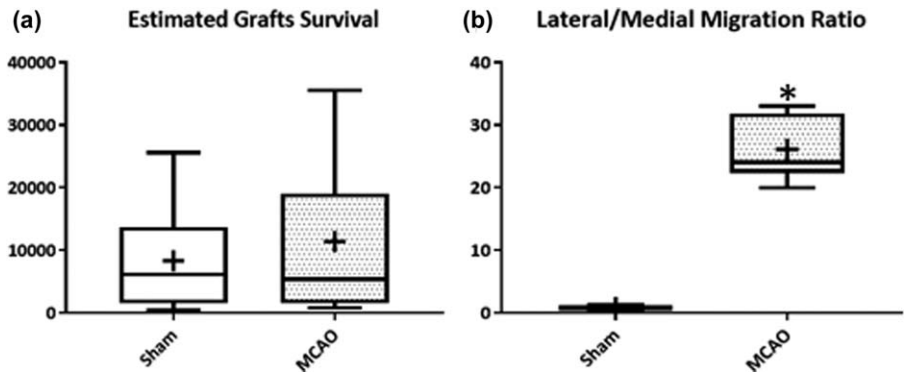


**FIGURE 4** Graft survival and migration profile. (a) Estimated graft survival. (b) Lateral/medial migration ratio. Plots represent whisker box plot. * $p < .0001$ ($t$ test, $n = 10$)

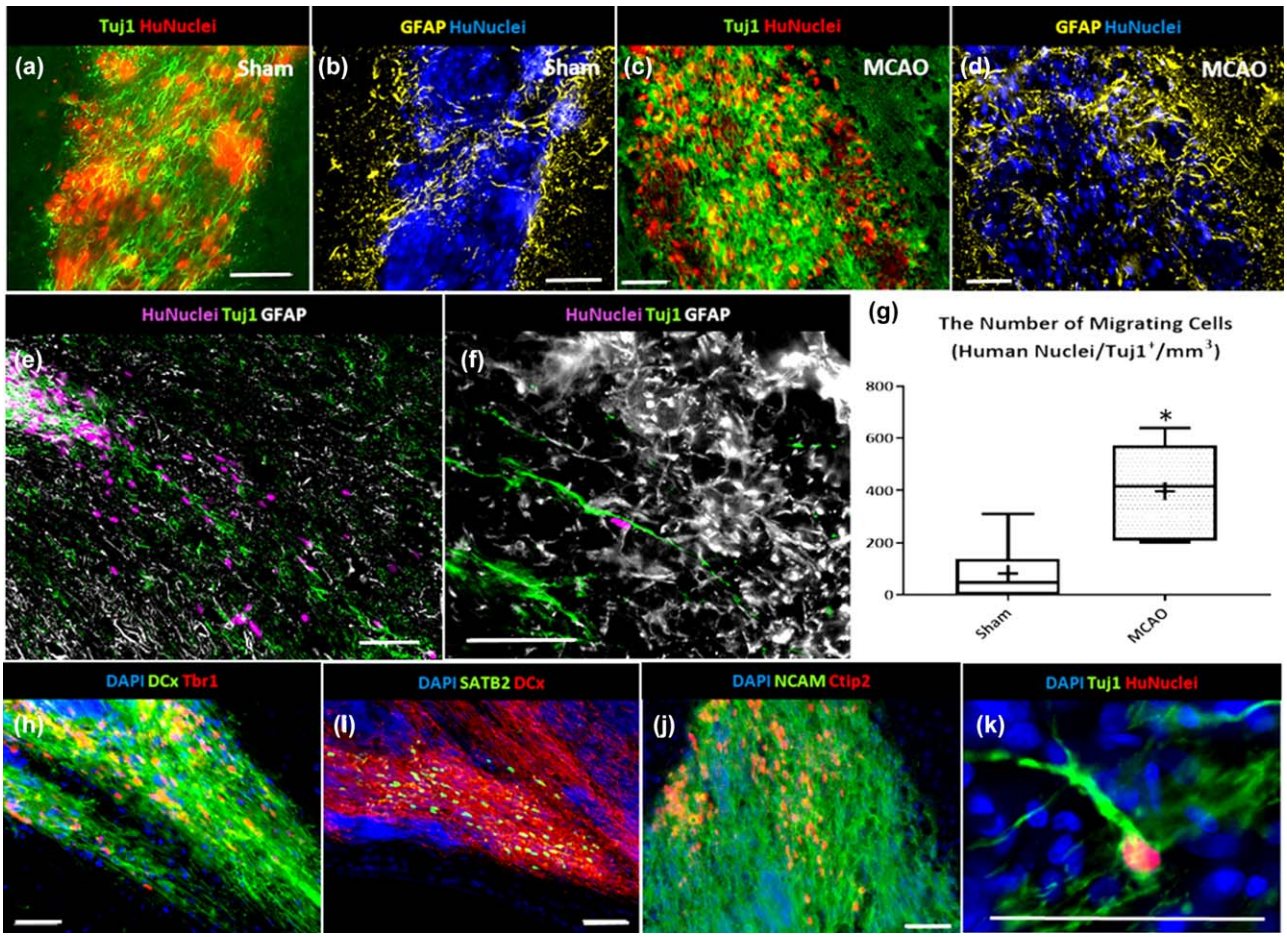


**FIGURE 5** Immunohistochemistry of graft characteristics. (a–d) The grafts' core consisted of $Tuj1^{+}/HuNuc^{+}$ and was surrounded by host gliosis ($GFAP^{+}/HuNuc^{-}$). (e) Immature neurons ($Tuj1^{+}/HuNuc^{+}$) migrated from the grafts' core. (f) None of the migrating cells differentiated into astrocytes even at the glial scar. (g) Grafts in MCAO exhibited more migration. (h–j) Grafts differentiated into the deep layer neurons of the neocortex (Tbr1, Ctip2, and Satb2). (k) A small proportion of migrating cells developed pyramidal-liked morphology. Scale bars: 50 μm. The graph represents whisker box plot. * $p = .0002$ (*t* test, $n = 10$). [Color figure can be viewed at wileyonlinelibrary.com]

cells were confirmed as immature neurons ($Tuj1^{+}/HuNuc^{+}$), and none of them differentiated into astrocytes ($GFAP^{+}/HuNuc^{+}$) (Figure 5e,f). There was no differentiation into oligodendrocyte lineages in either sham or MCAO rats. Migrating cells in MCAO were more numerous than in the sham group (398 ± 63 and 82 ± 32, respectively, $p = .0002$, *t* test) (Figure 5g). Transplanted cells differentiated into the deep layer neurons of the neocortex (Tbr1, Ctip2, and Satb2) (Figure 5h–j). A small proportion of migrating cells developed into pyramidal-neuron morphology after transplantation (Figure 5k).

## 3.3 | Axonal distribution

The axonal outgrowth in the sham group was minimum in density and short in distances (Figure 6a). In MCAO, the axon outgrowth was more robust and directed toward the ischemic border (Figure 6b). The optical density measurement confirmed the direction toward the ipsilesional side, in particular at the corpus callosum (0.0059 ± 0.0039 and 0.0558 ± 0.019, respectively, $p = .021$, *t* test) and nearby striatum (0.0056 ± 0.002 and 0.0004 ± 0.0002, respectively, $p = .025$, *t* test) (Figure 6c–e). The optical density at the other regions (contralesional corpus callosum and lateral septal nuclei) was indistinct (Figure 6f–j).

## 3.4 | hiPSC-derived cortical neuron progenitor transplantation enhances functional recovery and reduce microglia activation

Infarction yielded a remarkable sensorimotor impairment in adult male Wistar rats. The sensorimotor slowly recovered over time. In the aspect of vibrissae-evoked forelimb movement, functional recovery was indistinct (Figure 7a,b). Forelimb asymmetry in the cylinder test was better restored in transplanted rats at 1 month post transplantation (Figure 7c, $p = .0002$, 2-way ANOVA). Microglia activity increases at the glial scar after infarction, which is reflected by enhancement of Iba-1 immunoreactivity. There were fewer $Iba\text{-}1^{Hi+}$ cells in transplanted compared with vehicle-treated rats at 1 month post transplantation (84957 ± 8183 and 60582 ± 5364, respectively, $p = .0211$, *t* test) (Figure 8a–c). However, there is no statistical correlation between graft survival and the number of $Iba\text{-}1^{Hi+}$ in the ischemic cortex ($p = .1982$, linear regression).

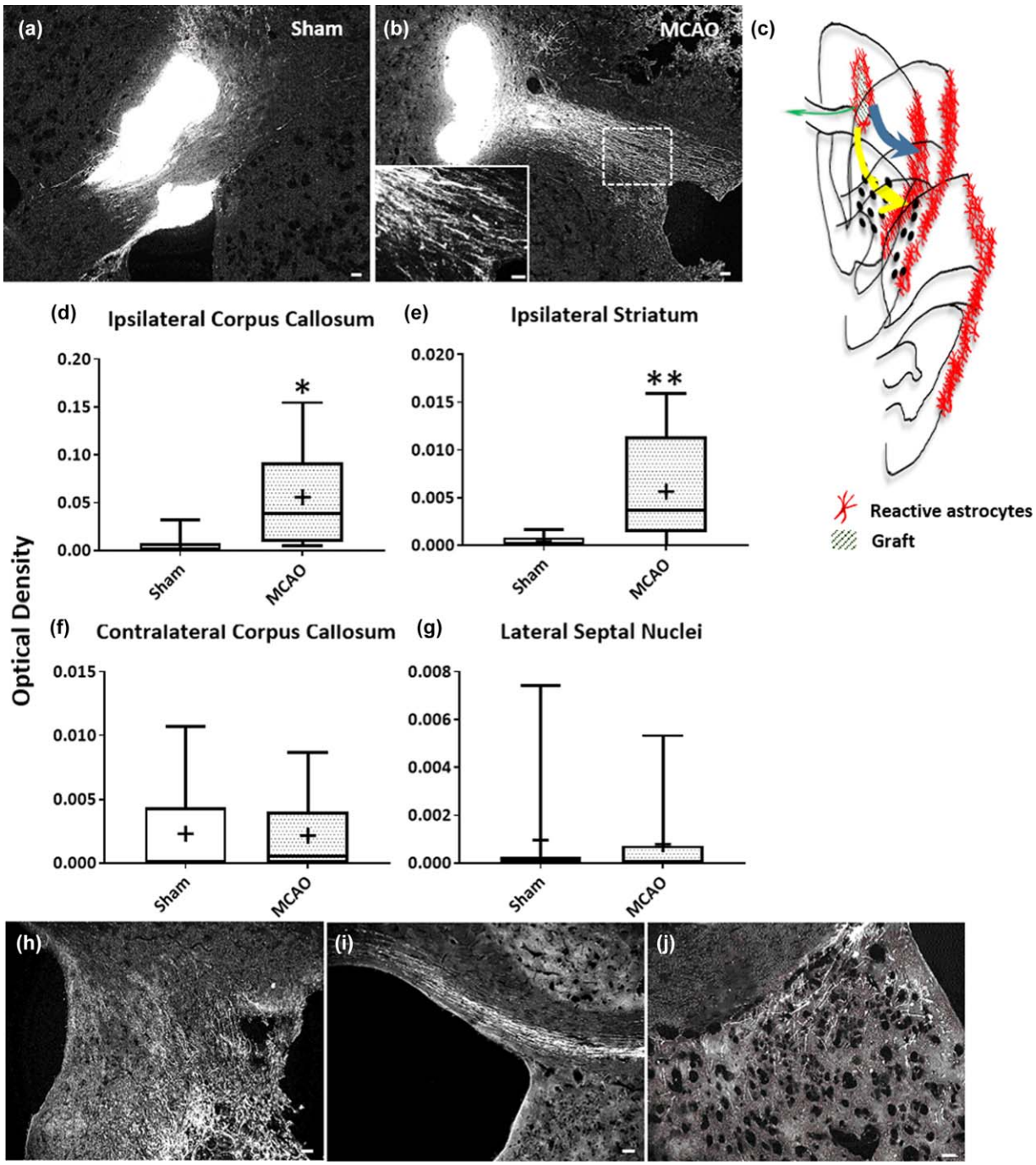


**FIGURE 6** Evaluation of grafts' axonal outgrowth with human NCAM antibody. (a,b) In the MCAO group, the axonal outgrowth was robust and directed toward the glial scar. (c) Schematic figure of axonal outgrowth directions in the MCAO brain. Blue arrow indicates ipsilesional corpus callosum, yellow arrow indicates ipsilesional striatum, and green arrow indicates contralesional corpus callosum. (d–g) The optical density measurement indicates the preference of the axonal outgrowth toward the ipsilesional side in the MCAO group. Axonal outgrowth was observed in the ipsilesional striatum (h), contralesional corpus callosum (i), and lateral septal nuclei (j). Scale bars: 50 μm. The graphs represent whisker box plots. * $p = .0214$, ** $p = .0248$ ($t$ test, $n = 10$). [Color figure can be viewed at wileyonlinelibrary.com]

## 4 | DISCUSSION

We obtained a comparable cortical neuron induction with previous feeder-maintained hiPSC neural induction (Gomi et al., 2012; Motono et al., 2016). The previous study showed that xeno-free neural induction could be performed with insulin, transferrin, and sodium selenite and taurine cocktail (Lukovic et al., 2017), but there was no cortical neuron formation. The majority of postmitotic neurons were GABAergic, which are physiological distinct from cortical neurons (glutamatergic) (Lukovic et al., 2017). The neuron is a highly specified cell that developed within the specific region of neuroaxis; therefore, each region yielded distinct neurons. The FoxG1 is indispensable for

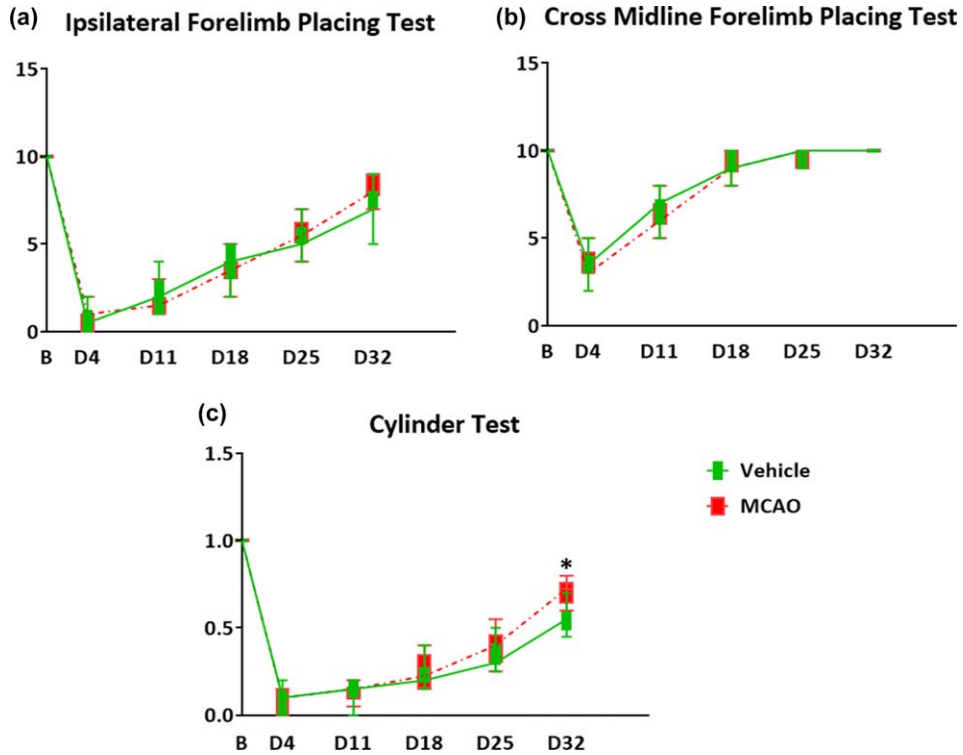


**FIGURE 7** Behavior testing. There is no significant behavior improvement on the forelimb placing test both ipsilateral (a) and cross-midline (b). Transplanted rats exhibited better performance than vehicle-treated rats on cylinder test after 1 month post transplantation. Graphs represent whisker box plot. * $p = .0002$ (2-way ANOVA, $n = 10$). [Color figure can be viewed at wileyonlinelibrary.com]

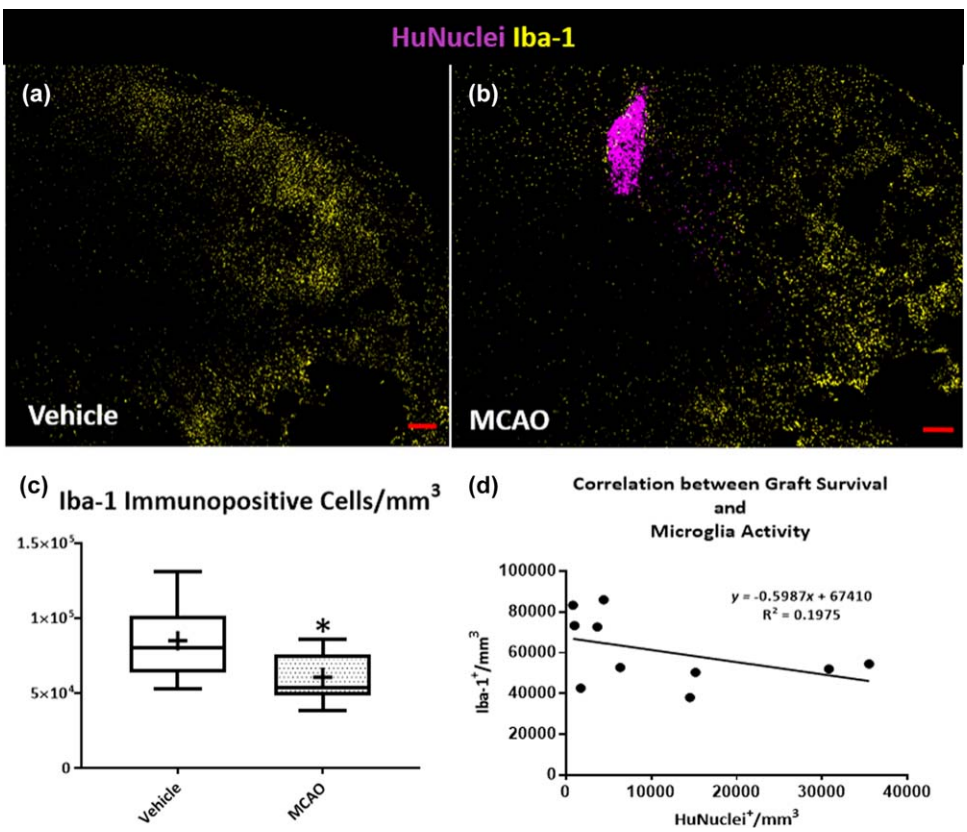


**FIGURE 8** Microglia activity after transplantation. (a–c) Transplantation reduces the number of Iba-$1^+$ cells at the ischemic border. (d) There is no statistical correlation between graft survival and Iba-$1^+$ cells at the ischemic cortex. Red scale bars: 200 μm. The graph represents whisker box plot. * $p = .0211$ ($t$ test, $n = 10$). [Color figure can be viewed at wileyonlinelibrary.com]

generation of the cortical neurons from hiPSCs; otherwise, the daughter cells will be different (Kadoshima et al., 2013). In this study, we applied the principle of dual-SMAD and Wnt inhibition to get specific telencephalon progenitor ($FoxG1^+/Pax6^+/Lhx2^+$) (Tao & Zhang, 2016). Of note, we found that there is clonal variability for induction of $FoxG1^+$ cells. In our experience, not all feeder-free clones generated FoxG1 under Wnt inhibition; some cell line was restricted to diencephalon progenitor ($Rax^+$). The neuroepithelial cells self-assembled in complex 3D architecture mimicking in vivo development. The newly born deep layer neurons resided at the periphery of the progenitor zone, which characterizes the initial cortical layer formation (Eiraku et al., 2008). One could further use the principle of embryoid-body induction for generation of brain organoids (Lancaster et al., 2013). Overall, the crucial step of cortical induction is the assurance of the pluripotency of PSCs and screening of suitable cell lines.

We did not detect any difference in graft survival upon transplantation either into sham or infarcted brain. Earlier reports also showed that the presence of ischemic damage in rats did not affect the survival of hiPSC-derived NSCs upon transplantation into the neurogenic zone in the subventricular zone (de la Rosa-Prieto et al., 2017). Tremendous migration and axonal outgrowth from the transplanted cells was noted particularly in the infarcted brain, which was directed toward the glial scar. Several reports indicated that this phenomenon could be mediated by chemoattractants as well as by other soluble factors in the ischemic border (Imitola et al., 2004; Kelly et al., 2004). The previous study also indicated that stroke environment alters grafted cells' axonal projection, in which grafted cells prefer the ischemic border rather than the rostral migratory system (De la Rosa Prieto et al., 2017).

In this study, the neuronal differentiation was unaffected by the ischemic environment. Ischemia promotes interleukin-6 (IL-6) expression in the ipsilesional hemisphere (Gertz et al., 2012), and IL-6–related protein is known as a strong inducer of gliogenesis in NSCs (Tsuyama et al., 2015). However, despite being attracted by and migrating toward the ischemic border, none of the cells in our grafts differentiated into astrocytes. Previous reports also yielded a high proportion of neurons and few glial cells (Andres et al., 2011; Espuny-Camacho et al., 2013; Gomi et al., 2012; Joannides et al., 2007; Mine et al., 2013; Oki et al., 2012; Tornero et al., 2013). The regional specification of NSCs is crucial for the temporal lineage specification. The dorsal part of the neuroaxis is known to have late onset of gliogenesis compared with the ventral part. Our cellular products express Pax6 and Lhx2, which represent the pallium lineage (neocortex), which has a later onset of gliogenesis. Therefore, our cells hinder the response to the gliogenic induction from the ischemic environment (Richardson, Kessaris, & Pringle, 2006).

Transplantation of cortical neuron progenitors better restores forelimb asymmetry in stroke rats compared with controls after 1 month of transplantation. Our evaluation indicated that transplantation did not reduce infarction sizes or promote endogenous neurogenesis (data not shown). The migration, neuronal differentiation, and axonal outgrowth toward the glial scar might contribute to the recovery process, as there were fewer $Iba\text{-}1^{Hi+}$ cells in the transplanted rats. There is a trend of negative correlation between poststroke inflammation and graft survival. The main confounding factor is immunosuppression (cyclosporine A); this might alter some inflammation or microglial profile behavior after stroke. Therefore, further study with immunocompromised rodents is necessary for confirmation.

We limit this study in adult male Wistar rats, to reduce infarct size variation. Female rodents are known to have smaller infarction and better neuroprotection than males (Manwani & McCullough, 2011). Ischemic stroke mainly affects the aging population; this population has lost the protective effect of gonadal steroids. Another option is a further evaluation on aging rodents.

To this end, our results prove that generation of transplantable hiPSC-derived cortical progenitors could be obtained from the feeder-free condition. Further studies are needed to find the biomolecular prediction of cell lines that are capable of differentiating into the telencephalon and improve clinical grade differentiation toward the xeno-free condition. Delayed transplantation into the chronic phase is more suitable for clinical translation. Hence, establishment of an animal model with a long-term neurological deficit is mandatory. Regarding that, we are developing a nonhuman primate model of focal brain ischemia for evaluation of clinical efficacy.

## CONFLICT OF INTEREST

The authors declare no conflicts of interest.

## AUTHOR CONTRIBUTIONS

All authors had full access to the data in the study and take responsibility for the integrity of the data and the accuracy of the data analysis. *Conceptualization*, Y.H. and Y.T.; *Methodology*, Y.H. and Y.T.; *Investigation*, Y.H. and T.S.; *Formal Analysis*, Y.H. and A.F.; *Resources*, J.T. and Y.T.; *Writing - Original Draft*, Y.H. and Y.T.; *Writing - Review & Editing*, Y.H., Y.T., and T.M.; *Supervision*, Y.T., J.T., S.M.; *Funding Acquisition*, J.T.

## ORCID

*Yulius Hermanto* http://orcid.org/0000-0003-2937-8130
*Takakuni Maki* http://orcid.org/0000-0001-9826-0203

## REFERENCES

Andres, R. H., Horie, N., Slikker, W., Keren-Gill, H., Zhan, K., Sun, G., … Steinberg, G. K. (2011). Human neural stem cells enhance structural plasticity and axonal transport in the ischaemic brain. *Brain*, *134*, 1777–1789.

Arvidsson, A., Collin, T., Kirik, D., Kokaia, Z., & Lindvall, O. (2002). Neuronal replacement from endogenous precursors in the adult brain after stroke. *Nature Medicine*, *8*, 963–970.

de la Rosa Prieto, C., Laterza, C., Gonzalez-Ramos, A., Wattanit, S., Ge, R., Lindvall, O., … Kokaia, Z. (2017). Stroke alters behavior of human skin-derived neural progenitors after transplantation adjacent to neurogenic area. *Stem Cell Research & #Therapy*, *8*, 59. https://doi.org/10.1186/s13287-017-0513-6

Doi, D., Samata, B., Katsukawa, M., Kikuchi, T., Morizane, A., Ono, Y., … Takahashi, J. (2014). Isolation of human induced pluripotent stem cell-derived dopaminergic progenitors by cell sorting for successful transplantation. *Stem Cell Reports*, *2*, 337–350.

Eiraku, M., Watanabe, K., Matsuo-Takasaki, M., Kawada, M., Yonemura, S., Matsumura, M., ... Sasai, Y. (2008). Self-organized formation of polarized cortical tissues from ESCs and its active manipulation by extrinsic signals. *Cell Stem Cell*, *3*, 519–532.

Espuny-Camacho, I., Michelsen, K. A., Gall, D., Linaro, D., Hasche, A., Bonnefont, J., ... Vanderhaeghen, P. (2013). Pyramidal neurons derived from human pluripotent stem cells integrate efficiently into mouse brain circuits in vivo. *Neuron*, *77*, 440–456.

George, P. M., & Steinberg, G. K. (2015). Novel stroke therapeutics: Unraveling stroke pathophysiology and its impact on clinical treatments. *Neuron*, *87*, 297–309.

Gertz, K., Kronenberg, G., Kallin, R. E., Baldinger, T., Werner, C., Balkava, M., ... Endres, M. (2012). Essential role of interleukin-6 in post stroke angiogenesis. *Brain*, *135*, 1964–1980.

Gomi, M., Takagi, Y., Morizane, A., Doi, D., Nishimura, M., Takahashi, J., & Miyamoto, S. (2012). Functional recovery of murine brain ischemia model using human induced pluripotent cell-derived telencephalic progenitors. *Brain Research*, *1459*, 52–60.

Imitola, J., Raddassi, K., Park, K. I., Mueller, F. J., Nieto, M., Teng, Y. D., ... Khoury, S. J. (2004). Directed migration of neural stem cells to sites of CNS injury by stromal cell-derived factor 1α/CXC chemokine receptor 4 pathway. *Proceedings of the National Academy of Sciences of the United States of America*, *101*, 18117–18122.

Joannides, A. J., Webber, D. J., Raineteau, O., Kelly, C., Irvine, K. A., Watts, C., ... Chandran, S. (2007). Environmental signals regulate lineage choice and temporal maturation of neural stem cells from human embryonic stem cells. *Brain*, *130*, 1263–1275.

Kalladka, D., Sinden, J., Pollock, K., Haig, C., McLean, J., Smith, W., ... Muir, K. W. (2016). Human neural stem cells in patients with ischaemic stroke (PISCES): A phase 1, first-in-man study. *Lancet*, *388*, 787–796.

Kadoshima, T., Sakaguchi, H., Nakano, T., Soen, M., Ando, S., Eiraku, M., & Sasai, Y. (2013). Self-organization of axial polarity, inside-out layer pattern, and species-specific progenitor dynamics in human ES cell-derived neocortex. *Proceedings of the National Academy of Sciences of the United States of America*, *110*, 20284–20289.

Kelly, S., Bliss, T. M., Shah, A. K., Sun, G. H., Ma, M., Foo, W. C., ... Steinberg, G. K. (2004). Transplanted human fetal neural stem cells survive, migrate, and differentiate in ischemic rat cerebral cortex. *Proceedings of the National Academy of Sciences of the United States of America*, *101*, 11839–11844.

Kondziolka, D., Steinberg, G. K., Wechsler, L., Meltzer, C. C., Elder, E., Gebel, J., ... Teraoka, J. (2005). Neurotransplantation for patients with subcortical motor stroke: A phase 2 randomized trial. *Journal of Neurosurgery*, *103*, 38–45.

Lancaster, M. A., Renner, M., Martin, C. A., Wenzel, D., Bicknell, L. S., Hurles, M. E., ... Knoblich, J. A. (2013). Cerebral organoids model human brain development and microcephaly. *Nature*, *501*, 373–379.

Lledo, P., Merkle, F. T., & Alvarez-Buylla, A. (2008). Origin and function of olfactory bulb interneuron diversity. *Trends in Neurosciences*, *31*, 392–400.

Lukovic, D., Lloret, A. D., Stojkovic, P., Rodriguez-Martinez, D., Arago, M. A. P., Rodriguez-Jimenez, F. J., ... Erceg, S. (2017). Highly efficient neural conversion of human pluripotent stem cells in adherent and animal-free conditions. *Stem Cells Translational Medicine*, *6*, 1217–1226.

Manwani, B., & McCullough, L. D. (2011). Sexual dimorphism in ischemic stroke: Lessons from the laboratory. *Women's Health*, *7*, 319–339.

Meng, G., Liu, S., & Rancourt, D. E. (2011). Synergistic effect of medium, matrix, and exogenous factors on the adhesion and growth of human pluripotent stem cells under defined, xeno-free conditions. *Stem Cells and Development*, *21*, 2036–2048.

Mine, Y., Tatarishvilli, J., Oki, K., Monni, E., Kokaia, Z., & Lindvall, O. (2013). Grafted human neural stem cells enhance several steps of endogenous neurogenesis and improve behavioral recovery after middle cerebral artery occlusion in rats. *Neurobiology of Disease*, *52*, 191–203.

Moskowitz, M. A., Lo, E. H., & Iadecola, C. (2010). The science of stroke: Mechanisms in search of treatments. *Neuron*, *67*, 181–198.

Motono, M., Ioroi, Y., Ogura, T., & Takahashi, J. (2016). Wnt-C59, a small-molecule wnt inhibitor, efficiently induces anterior cortex that includes cortical motor neurons from human pluripotent stem cells. *Stem Cells Translational Medicine*, *5*, 552–560.

Oki, K., Tatarishvilli, J., Wood, J., Koch, P., Wattananit, S., Mine, Y., ... Kokaia, Z. (2012). Human-induced pluripotent stem cells form functional neurons and improve recovery after grafting in stroke-damaged brain. *Stem Cells*, *30*, 1120–1133.

Richards, M., Fong, C. Y., Chan, W. K., Wong, P. C., & Bongso, A. (2002). Human feeders support prolonged undifferentiated growth of human inner cell masses and embryonic stem cells. *Nature Biotechnology*, *20*, 933–936.

Richardson, W. D., Kessaris, N., & Pringle, N. (2006). Oligodendrocyte wars. *Nature Reviews Neuroscience*, *7*, 11–18.

Schallert, T., Fleming, S. M., Leasure, J. L., Tillerson, J. L., & Bland, S. T. (2000). CNS plasticity and assessment of forelimb sensorimotor outcome in unilateral rat models of stroke, cortical ablation, parkinsonism and spinal cord injury. *Neuropharmacology*, *39*, 777–787.

Takagi, Y., Tokime, T., Nozaki, K., Gon, Y., Kikuchi, H., & Yodoi, J. (1998). Redox control of neuronal damage during brain ischemia after middle cerebral artery occlusion in the rat: Immunohistochemical and hybridization studies of thioredoxin. *Journal of Cerebral Blood Flow and Metabolism*, *18*, 206–214.

Takahashi, K., Tanabe, K., Ohnuki, M., Narita, M., Ichisaka, T., Tomoda, K., & Yamanaka, S. (2007). Induction of pluripotent stem cells from adult human fibroblasts by defined factors. *Cell*, *131*, 861–872.

Tao, Y., & Zhang, S. C. (2016). Neural subtype specification from human pluripotent stem cells. *Cell Stem Cell*, *19*, 573–586.

Tornero, D., Wattanit, S., Gronning Madsen, M., Koch, P., Wood, J., Tatarishvilli, J., ... Kokaia, Z. (2013). Human induced pluripotent stem cell-derived cortical neurons integrate in stroke-injured cortex and improve functional recovery. *Brain*, *136*, 3561–3577.

Tsuyama, J., Bunt, J., Richards, L. J., Iwanari, H., Mochizuki, Y., Hamakubo, T., ... Okano, H. (2015). MicroRNA-153 regulates the acquisition of gliogenic competence by neural stem cells. *Stem Cell Reports*, *5*, 365–377.

Woodlee, M. T., Asseo-Garcia, A. M., Zhao, X., Liu, S. J., Jones, T. A., & Schallert, T. (2005). Testing forelimb placing "across the midline" reveals distinct, lesion-dependent patterns of recovery in rats. *Experimental Neurology*, *191*, 310–317.

Zhang, D., Mai, Q., Li, T., Huang, J., Ding, C., Jia, M., ... Xu, Y. (2016). Comparison of a xeno-free and serum-free culture system for human embryonic stem cells with conventional culture systems. *Stem Cell Research & Therapy*, *7*, 101. https://doi.org/10.1186/s13287-016-0347-7

**How to cite this article:** Hermanto Y, Sunohara T, Faried A, et al. Transplantation of feeder-free human induced pluripotent stem cell–derived cortical neuron progenitors in adult male Wistar rats with focal brain ischemia. *J Neuro Res*. 2018;96:863–874. https://doi.org/10.1002/jnr.24197